# Utilizing functionalized bromomaleimides for fluorogenic conjugation and PEGylation of enzymes

Husband, J.T.; Hill, A.C.; O'Reilly, R.K.

*DOI:*
10.1002/pi.5740

# Utilizing functionalized bromomaleimides for fluorogenic conjugation and PEGylation of enzymes

Jonathan T. Husband,[a] Alice C. Hill [b] and Rachel K. O'Reilly [a]*

[a] School of Chemistry, University of Birmingham, Edgbaston, Birmingham, B15 2TT, United Kingdom
[b] Department of Chemistry, University of Warwick, Gibbet Hill Road, Coventry CV4 7AL, United Kingdom

**ABSTRACT:** Two efficient enzyme conjugation techniques have been explored by exploiting the reactions of bromomaleimides. The conjugations utilize monobromo- and dibromo- maleimides, which have been reacted with reduced disulfide bonds or terminal amines in α-chymotrypsin and human lysozyme. These reactions allow the formation of dithio- (DTM), monoamino- (MAM), and aminobromo- (ABM) maleimides, which are solvent-dependent fluorophores and have a handle for further functionalization, which allowed fluorogenic PEGylation *via* this technique. In this work, the efficiency of these maleimide conjugations was monitored and the fluorescence of the resulting conjugates have been examined. The quantum yields of the small molecule maleimide conjugates have been calculated, but are low due to solvent quenching effects. Catalytic activities of the conjugate enzymes have been compared to their respective native enzymes, which show no discernible effect of the modifications on enzymatic activity or stability at room temperature.

**Keywords:**
Enzyme, PEGylation, fluorescence, maleimide

## INTRODUCTION

Fluorescent labelling of proteins is a widespread practice. It is used for many applications, including visualizing intracellular trafficking,(1) tracking cellular uptake,(2,3) measuring conformational changes,(4–6) and environmental sensing.(7) Commonly this is achieved by conjugating fluorescent proteins to the target.(8) Not only may the large size of such proteins have a significant effect on the properties/function of the target, but they are prone to photobleaching.(9,10) Another strategy is to conjugate a small molecule fluorophore to the studied protein *via* an amino acid residue.(11,12) Often this is achieved though the complex process of incorporating a non-natural amino acid into the protein through genetic expression, which can be selectively conjugated.(13–15) In unmodified enzymes the two most commonly accessed sites for labelling are lysine and cysteine residues, which can be utilized if minimal site specificity is required.(16)

In addition to fluorescent labelling, conjugation to enzymes is frequently utilized for the attachment of poly(ethylene glycol) (PEG) to therapeutic targets, called PEGylation. PEGylation can enhance the therapeutic properties of a molecule. This can include better physical and thermal stability,(17) protection against degradation,(18) increased solubility,(19) longer half-life *in vivo*,(20) and even increased potency.(21) As of 2013, there were nine PEGylated proteins approved by the FDA for pharmaceutical use.(22) All of these are conjugated *via* either lysine residues, the *N*-terminus or cysteine residues.(22)

Cysteine is regarded as the most nucleophilic amino acid in the majority of proteins and therefore is commonly regarded as the easiest to modify. The most widely used cysteine modification technique is maleimide conjugation; in which cysteine will undergo a highly selective addition to the maleimide double bond.(23,24) This technique has been utilized for the creation of responsive polymer-protein bioconjugates,(25) for PEGylation,(26) target specific fluorescent labelling,(27) and the radiolabeling of proteins.(28) In recent literature, it has been shown that monobromomaleimides (MBM) and dibromomaleimides (DBM) also undergo efficient, selective reactions with cysteine residues.(29,30) In comparison to maleimide conjugations, the double bond of the maleimide is retained and hence the reaction is reversible. This has led to applications in antibody conjugations, where the reaction of two reduced cysteines with dibromomaleimide forms a bridged dithiomaleimide (DTM) conjugate. (31–33) The bridging of disulfides using DBMs has been optimized to provide a high yielding, site-selective method for drug-antibody conjugation, allowing control over drug loading. By linking trastuzumab with antibody monomethyl auristatin E *via* a DTM linker, Nunes *et. al.* synthesized an antibody-drug conjugate (ADC), which showed cancer cell selectivity and excellent potency *in vitro*.(34) Haddleton and co-workers have applied this technique to salmon calcitonin, a small helical peptide,(35) and oxytocin, a therapeutic cyclic peptide which helps reduce postpartum hemorrhaging.(36,37) When PEG is conjugated to oxytocin using this technique, the solution stability of the peptide was greatly improved, however effects on *in vivo* activity have not been reported. The technique has also recently been reported as a peptide stapling method to stabilize α-helices and help prevent proteolysis.(38)

In addition to their use in disulfide bridging, DTMs have been proven to be a class of highly emissive fluorophore.(35) It has been shown that the solubility and further functionalization of DTMs could be easily varied through selection of N- and S- substituents. Generally, the fluorophore has bright solvent-dependent emission,

around 500 nm in dioxane, with polar protic solvents causing a red shift and quenching of emission. The fluorescence has also been demonstrated to be quenched by aromatic thiol substitution (e.g. dithiophenolmaleimide).(39) The dye has found applications in polymer research after the supramolecular assembly of DTM-functionalized polymers was shown to dictate emissivity, emission polarization, and fluorescence lifetime.(35,39–43) This has been attributed to the polymeric scaffold preventing both solvent and collisional quenching effects. *In vivo* studies of DTM polymers enabled differentiation of the micellar and unimeric species, based on fluorescence lifetime imaging microscopy (FLIM), as a consequence of the shorter fluorescence lifetimes of the unimeric species.(39) The presence of a DTM dye also allows detection of guest molecules by Förster resonance energy transfer (FRET).(44)

In the meantime, it has been shown that monoaminomaleimides (MAMs) and aminobromomaleimides (ABMs), which are synthesized by addition–elimination reactions with MBM and DBM respectively, are also highly emissive.(45) These moieties have large Stokes shifts (~100 nm) and show solvent-dependent emission wavelengths and intensities, with polar protic solvents causing a red shift and large reduction in emission intensity. In parallel to DTMs, they are also quenched by direct conjugation of aromatic amines to the maleimide ring, but these arylaminomaleimides have been shown to exhibit aggregation induced fluorescence in the solid state.(46,47) We proposed, based on bromomaleimide conjugations with cysteine, that a conjugation induced fluorescence technique could be realized utilizing lysine residues. Amine-reactive conjugation techniques are often used for conjugations, most frequently through *N*-hydroxysuccinimide (NHS) activated esters or 1-ethyl-3-(3-dimethylaminopropyl)carbodiimide (EDC) coupling.(16,48) These techniques require activation of a carboxylic acid group prior to conjugation through additives, and as a result of the large number of lysine residues usually present in proteins, it is typically difficult to control the location and number of modifications.(48) A fluorogenic technique that is high yielding and requires no additives or activation, could offer an attractive alternative approach to the conjugation of large fluorescent dyes or fluorescent proteins as used in many current applications,(49) and would provide a fluorogenic PEGylation method.

In addition to their fluorescence properties, it is important to consider the effect of bromomaleimide conjugations on protein structure and enzymatic function. In previous research DTMs have not been conjugated specifically to functional enzymes, but they have been conjugated to peptides, for example salmon calcitonin(50) and oxytocin(36,37) however, the effect on activity of these peptides

has not been studied. Therefore, it is unknown whether the initial activity or long term stability of a therapeutic peptides or an enzyme would be impacted through the introduction of these moieties upon conjugation. It is hypothesized that the bridging of disulfide bonds with a maleimide moiety could introduce additional stability, through preventing disulfide reduction. This study will investigate the formation of functionalized MAMs, ABMs and DTMs in enzyme conjugations and how the substituents affect the integrity of two enzymes, α-chymotrypsin (α-CT) and human lysozyme (HLZ), which are enzymes commonly used in conjugation based applications and have been extensively characterized.(51–58)

## MATERIALS AND METHODS

α-chymotrypsin (Type II from bovine pancreas, lyophilized powder) and human lysozyme (expressed in rice, lyophilized powder) were used as received from Sigma-Aldrich and stored in a freezer at approximately -18 °C. All other chemicals were obtained from either: Sigma Aldrich, Fisher Chemicals, Acros Chemicals, Alfa Aesar or IRIS biotech GmbH and used as received.

### 2-3-dibromo-pyrrole-2,5-dionefunctionalized $PEG_{350}$ (1)

Triphenyl phosphine (1.44 g, 5.5 mmol) was dissolved in dry tetrahydrofuran (100 mL) and cooled to -78 °C. Diisopropyl azodicarboxylate (1.14 mL, 5.5 mmol) was added dropwise and the solution was left to stir for 5 minutes. Methoxypoly(ethylene glycol) ($M_n$= 350 g/mol, 1.75 g, 5.5 mmol) was added dropwise to the cooled solution and left to stir for a further 5 minutes. Neopentyl alcohol (0.22 g, 2.5 mmol) was added and left to stir for a further 10 minutes. 3,4-dibromomaleimide (1.39 g, 5.5 mmol) was added to the solution and left to stir at -78 °C for 1 hour. The solution was allowed to warm to room temperature and left to stir for 24 hours. The solvent was removed *in vacuo,* and the resultant oil purified by silica column by flash chromatography (2:1 to 0:1 gradient of petroleum ether 40-60°C : EtOAc) to yield a yellow oil **1** (287 mg, 17 %). $R_f$ (2:1 petroleum ether 40-60°C : EtOAc): 0.1 to 0.4.

$^1$H NMR ($CDCl_3$, 300MHz, ppm)- δ 3.82 (t, $^3J_{H-H}$= 5.6Hz, 2H, NC$H_2$), 3.71-3.53 (br m, 31H, C$H_2$-$CH_2$), 3.38 (s, 3H, C$H_3$-O).

$^{13}$C NMR ($CDCl_3$, 125MHz) $\delta$ (ppm) = 163.8, 129.4, 71.9, 70.6-70.5, 70.1, 67.5, 59.0, 38.9

HR-MS (MaXis) - $[M+Na]^+$ calculated m/z 688.0764, observed m/z 688.0768

FTIR ($cm^{-1}$) –2872 ($\upsilon_{C-H}$), 1716 ($\upsilon_{C=O}$), 1104 ($\upsilon_{C-O}$)

### Synthesis of 3-bromo-1-methyl-1H-pyrrole-2,5-dione (2)

The synthesis was based on a previously reported literature procedure.(59) To a solution of bromomaleic anhydride (1 g, 5.65 mmol) in acetic acid (20 mL) was added methyl amine in ethanol (695 µl, 5.65 mmol). The solution was refluxed for 3 hours after which the solvent was removed *in vacuo*. The resultant solid was purified by silica column chromatography and eluted with 10% ethyl acetate in petroleum ether 40-60 °C to give a cream colored solid **2** (190 mg, 15 %). $R_f$: 0.2

$^1$H NMR ($CDCl_3$, 500 MHz) $\delta$ (ppm) = 6.88 (s, 1H, C*H*CBr), 4.33 (s, 3H, NC$H_3$).

MS (ESI) - $[M+H]^+$: observed: 190.0 calculated: 189.9

Matches literature data.(59)

**Synthesis of 3-bromo-1-(prop-2-yn-1-yl)-1H-pyrrole-2,5-dione (3)**

The synthesis was based on a previously reported literature procedure.(59) To a solution of bromomaleic anhydride (1.2 g, 6.9 mmol) in acetic acid (15 mL) was added propargyl amine (432 µl, 7.5 mmol). The solution was refluxed for 6 hours after which the solvent was removed *in vacuo*. The resultant solid was purified by silica column chromatography and eluted with 100% dichloromethane ($CH_2Cl_2$) to give a cream colored solid **3** (1.1 g, 78 %). $R_f$ (100% $CH_2Cl_2$): 0.9

$^1$H NMR ($CDCl_3$, 300MHz) $\delta$ (ppm) = 6.39 (s, 1H, C*H*CBr), 4.33 (d, $^4J_{H\text{-}H}$= 2.5Hz, 2H, NC$H_2$) and 2.24 (t, $^4J_{H\text{-}H}$= 2.5Hz, 1H, *H*C≡C).

$^{13}$C NMR ($CDCl_3$, 75MHz) $\delta$ (ppm) = 167.1, 162.1, 132.2, 131.7, 76.4, 72.1 and 27.8.

HR-MS (MaXis) - $[M+Na]^+$ calculated m/z 235.9318, observed m/z 235.9316

FTIR ($cm^{-1}$) – 3271 ($\upsilon_{H\text{-}C\equiv C}$), 1702 ($\upsilon_{C=O}$), 1687 ($\upsilon_{C=O}$).

Elemental analysis found: C 39.23, H 1.80, N 6.48; expected ($C_7H_4BrNO_2$): C 39.29, H 1.88, N 6.54.

**3-bromo-pyrrole-2,5-dionefunctionalized $PEG_{800}$ (4)**

Methoxy-poly(ethylene glycol)-$amine_{800}$ ($M_n$= 800 g/mol, 0.48g, 0.6 mmol) was added to 15ml of acetic acid. Bromomaleic anhydride (0.13 g, 0.75 mmol) was added and the solution was refluxed overnight. The solvent was removed *in vacuo* and the resultant orange oil purified by flash chromatography on a silica column (2:1 $CH_2Cl_2$ : Methanol) to give a viscous oil **4** that was >90 % functionalized according to $^1$H NMR spectroscopy (0.403 g, 67 %). $R_f$ (2:1 $CH_2Cl_2$ : Methanol): 0.05-0.35.

$^1$H NMR ($CDCl_3$, 300MHz)- $\delta$ (ppm) 6.88 (s, 0.9H, C*H*CBr), 3.77 (t, $^3J_{H\text{-}H}$ = 5.4Hz, 2H, NC$H_2$), 3.68-3.53 (br m, 76H, C$H_2$-$CH_2$), 3.38 (s, 3H, C$H_3$-O).

$^{13}$C NMR ($CDCl_3$, 500MHz, ppm)-168.4, 156.2, 132.0, 131.4, 71.9, 70.6-70.5 (m), 70.1, 67.7, 38.08

HR-MS (MaXis) - $[M+Na]^+$ calculated m/z 872.3250, observed m/z 872.3257

FTIR ($cm^{-1}$) – 2824 ($\upsilon_{C\text{-}H}$), 1720 ($\upsilon_{C=O}$), 1106 ($\upsilon_{C\text{-}O}$)

**General procedure for dithiomaleimide conjugations**

3 mg of enzyme was dissolved in 1.3 mL 0.1 M pH 6 Phosphate buffer, followed by addition of 0.1 mL *tris*(2-carboxyethyl)phosphine (TCEP) solution (4 equivalents per disulfide, in 18.2 MΩ.cm water). The reaction was vortexed and left to stir for 30 minutes. After this, 0.1 mL of DBM solution (5 equivalents per disulfide, in DMF) was added and the mixture vortexed. Maximum degree of conjugation, identified by MALDI-ToF MS, was reached after 30-60 minutes. The crude enzyme was purified by ultrafiltration (AMICON® stirred cell), freeze-dried and analyzed by MALDI-ToF.

**General procedure for aminomaleimide conjugations**

3 mg of enzyme was dissolved in 1 mL of 0.1 M pH 8.5 Tris buffer. 0.5 mL DBM solution (5 equivalents per amine in DMF) was added and the solution vortexed. Maximum degree of conjugation, identified by MALDI-ToF MS, was reached after leaving overnight. The crude enzyme was purified by ultrafiltration, freeze-dried and analyzed by MALDI-ToF.

**α-Chymotrypsin *p*-nitroaniline hydrolysis assay**

Activity and stability of the enzyme and conjugates were assessed by analysis of the initial velocity changes in absorbance with time. Native αCT and conjugates (2 μg/ml) were incubated in 0.1 M sodium phosphate buffer (pH 6) at 4 °C. 20 μL aliquots of these solutions were added to 160 μL of 0.1M sodium phosphate buffer (pH 6) in a 96 well plate and 20 μL of *N*-Succinyl-Ala-Ala-Pro-Phe p-nitroanilide in methanol (3 mg/ml) was added. Each sample was run in triplicate against buffer blanks. The initial rate of hydrolysis of the substrate was monitored through recording the rate of increase in absorption at 405 nm at 25 °C over 30 minutes. Background hydrolysis was subtracted to give initial rates of hydrolysis.

**Human lysozyme EnzCheck® lysis assay**

Lysozyme assays were carried out as reported in the literature.(60) Lysozyme substrate stock suspension (1.0 mg/ml) was prepared according to the manufacturer, and aliquots were diluted to 50 mg/ml for each assay. Prior to conjugate analysis, the substrate was used to generate a standard curve. 6 wells of a 96 well plate were filled with 50 μL of 0.1 M sodium phosphate buffer (pH 6) followed by a solution of 50 μL 500 U/mL of human lysozyme solution was added to the first well. The solutions were mixed and 50 μL was transferred into a second well. This was repeated over 5 wells, with the final 50 μL from the 5$^{th}$ well discarded. To these solutions, 50 μL of the 50 mg/ml substrate solution was added. These solutions in triplicate were incubated at 37 °C in a plate reader and emission at 530 nm (excitation at 492 nm) was recorded *vs.* time. From this, a value of 62.5 U/ml

was identified as the concentration for future assays. For the stability assay, Native human lysozyme and conjugates (2 mg/ml) were incubated in 0.1 M sodium phosphate buffer (pH 6) at 4 °C. Aliquots of these solutions were diluted to 5 µg/ml and 50 µL of these solutions was pipetted onto a 96 well plate. To these solutions, 50 µL of the 50 mg/ml substrate solution was added and these solutions, in triplicate, incubated at 37 °C in a plate reader. Analysis was carried out by measuring emission at 530 nm after 30 minutes, as per the manufacturer's protocol. Errors were measured as a standard deviation over all time points for each triplicate.

**Quantum yield fluorescence analysis**

Quantum yield analysis was based on a previously reported literature procedure.(61) A solution of quinine sulfate dihydrate (15 µmol) in 0.105 M perchloric acid, was used a standard (Φquinine = 59 %), from which a UV-Vis spectrum was recorded.

The conjugate of interest was diluted to a concentration affording an absorbance <0.1 at the excitation wavelength determined by UV-Vis analysis. Both spectra were overlaid, and the optimal excitation wavelength for the calculation was chosen to be the wavelength where the standard and the sample have the same absorption. Using the excitation wavelength for fluorescence, the emission of both samples was measured. To calculate the quantum yield Equation 1 is used, where F= Integral photon flux (emission integral), f= absorbance, n=refractive index of the solvent, $\lambda_{em}$= emission wavelength, conj=conjugate sample, and st=quinine standard.

$$\text{Equation 1: } \Phi_{f,conj} = \Phi_{f,st} \cdot \frac{F_{conj}}{Fst} \cdot \frac{f_{st}}{f_{conj}} \cdot \frac{n^2_{conj}(\lambda_{em})}{n^2_{st}(\lambda_{em})}$$

As the absorbance for the standard and sample match, it can be neglected ($f_{st}/f_{conj}$=1). Refractive indices are found for the conjugate and quinine solvents at their respective average emission wavelengths (wavelength corresponding to the mean of the emission spectrum integration). The standard quantum yield $\Phi_{f,st}$($\Phi_{quinine}$= 59 %) was used to calculate the relative fluorescence of each conjugate.

**Instrumentation**

NMR spectra were recorded on a Bruker Avance 300, a Bruker Avance III HD 400 or a Bruker Avance III HD 500 spectrometer at 298k and 300, 400 and 500 MHz respectively. Shifts are quoted in $\delta$ in parts per million and quoted relative to the internal standard trimethylsilane (TMS). High Resolution Mass Spectra (HR-MS) were conducted on a Bruker UHR-Q-ToF MaXis spectrometer with electrospray ionization. MALDI-ToF MS was conducted on a Bruker Autoflex MALDI TOF/TOF spectrometer. For MALDI analysis protein solution (2.0 mg/ml) was spotted on the MALDI plate

followed by an equal volume of sinapinic acid matrix (15 mg in 0.5 mL of water, 0.5 mL of acetonitrile and 1 µL of trifluoroacetic acid (TFA). The solvent was evaporated before the recording of spectra and analysis using FlexControl software. Gaussian fits were completed on aminomaleimide conjugates which could be successfully fitted and full width at half maximum (FWHM) analysis was used to determine the standard deviation (FWHM = 2.355*σ). It should be noted that MALDI-ToF MS analysis of native HLZ showed a strong signal at around 14110 m/z, which does not match literature structures of HLZ, but has been observed by other groups.(62) However, the secondary peak at 14692 m/z correlates well with published structures and therefore conjugation mass shifts were based on this value.

Infrared spectra were recorded on neat samples using a Perkin Elmer Spectrum 100 FT-IR Spectrometer. UV-Vis spectroscopy was carried out on a Perkin Elmer Lambda 35 UV-Vis spectrometer or an Agilent Cary 60 UV-Vis Spectrometer at room temperature. Fluorescence spectra were recorded using an Agilent Cary Eclipse Fluorescence spectrophotometer. Quartz cells with four polished sides (Starna) were used for fluorescence and UV-Vis measurements. Enzyme assays were conducted on a FLUOstar OPTIMA multi-well microplate reader according to the assay conditions for each individual enzyme.

Differential scanning calorimetry (DSC) analysis was performed on a TA instruments Nano DSC. Blank runs were ran with buffer in both sample and reference side. Each protein sample was run with buffer in the reference side. Scans were made between 20 and 100 °C at 1 °C/min and a 600 s equilibration time was applied prior to each the scan. Circular dichroism (CD) spectra were recorded on a J-720 CD spectrometer in 1 mM pH 6.0 phosphate buffer using a quartz cuvette with a path length of 0.1 cm. All experiments were run with ten acquisitions and recorded at 20 nm/min. The molar ellipticity was based off protein concentration measured at 280 nm.

## RESULTS AND DISCUSSION

To study disulfide re-bridging on enzymes the five disulfide bonds of α-CT were targeted as handles for conjugation. *N*-methyldibromomaleimide (M-DBM) was chosen as the initial conjugating molecule, due to its small size and reported resistance to hydrolysis,(44) and tris(2-carboxyethyl)phosphine (TCEP) was used to reduce the disulfides prior to conjugation (Figure 1A). Unusually for disulfide based conjugations, reacting M-DBM under an optimized protocol produced a singular conjugate with three DTMs conjugated (Figure 1C) as observed by matrix-assisted laser desorption/ionization-time of flight mass spectroscopy (MALDI-ToF MS). This suggests that two of the disulfides are not solvent accessible and therefore under such conditions this conjugation technique can produce site-specific conjugates.

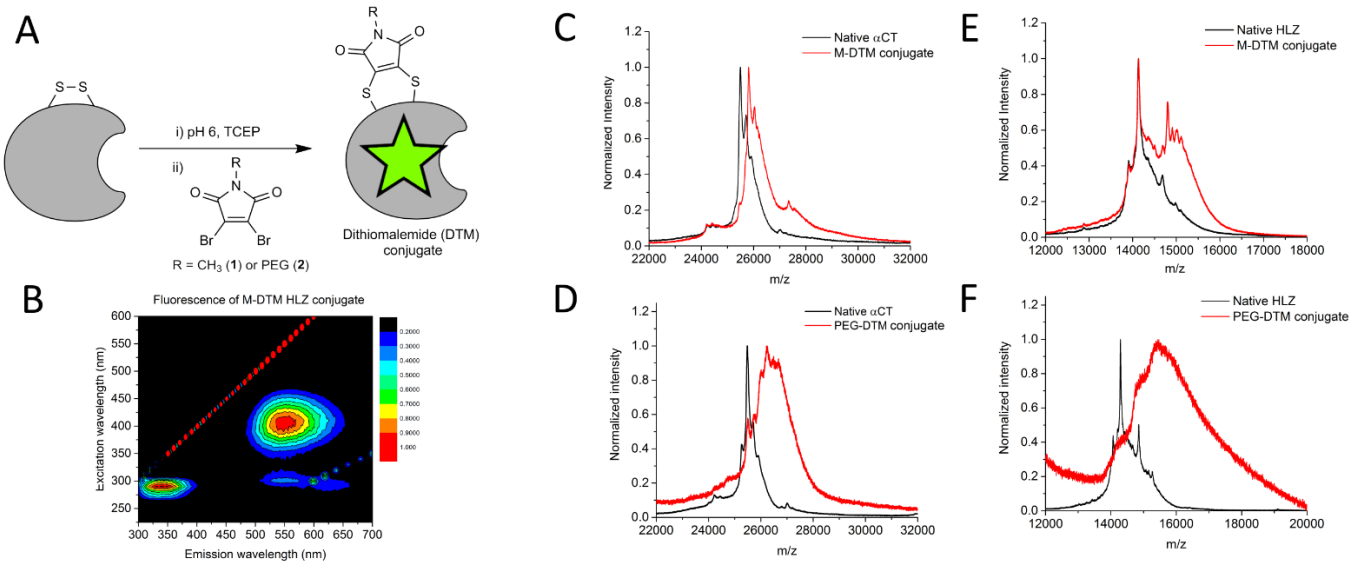


**Figure 1:** (A) Illustration of disulfide based bromomaleimide conjugations to α-CT and HLZ. (B) 2D excitation–emission spectra of M-DTM HLZ conjugate. MALDI-ToF mass spectra of (C) M-DTM α-CT conjugate (D) PEG-DTM α-CT conjugate (E) M-DTM HLZ conjugate (F) PEG-DTM HLZ conjugate (red) with the native enzyme (black).

To confirm this, analysis of the availability of the disulfides in αCT was undertaken. Firstly, a Kyte-Doolittle plot was drafted to establish if any of the disulfides were located in a particularly hydrophobic location in the enzyme, which may be buried and therefore inaccessible for conjugation. (Figure S15). While the disulfide C168-C182 appears to be the most hydrophobic – and therefore least likely to be reacted - and disulfide C191-C220 appears to be the most hydrophilic, no other conclusions could be drawn. To gain further insight the solvent accessible surface

area of the enzyme was calculated using a crystal structure of the enzyme (from the Protein Data Bank: 4CHA).(52) It was clear that C191-C220 had the most solvent accessible surface area (Table S1) by this model, and C168-C182 and C191-220 displayed minimal to no solvent accessible surface area. This is in concurrence with the hydrophobicity plot, suggesting that the C1-C122 bond is very likely to be the most reactive disulfide, and that the C168-C182 and C191-220 bonds are the unmodified bonds. A trypsin digest was attempted to prove this hypothesis, however as a consequence of α-CT autolysis this was not informative.

To ascertain that the bromomaleimide conjugations are applicable to a range of enzymes, human lysozyme was chosen as a second target for conjugation. Human lysozyme (HLZ) has four disulfide bonds as handles for attachment, is smaller than α-CT and does not perform autolysis.(54) Disulfide bridging to HLZ using M-DBM was undertaken using the same conditions as for α-CT. In contrast to α-CT, a distribution of 0-4 DTM species were observed by MALDI-ToF MS after purification (Figure 1E). Interestingly, up to four DTMs can be formed per enzyme suggesting that all are solvent accessible, which may be a result of the more hydrophilic nature of HLZ. However, as often observed in multi-site conjugation techniques,(57) only a distribution of differentially conjugated products was obtainable, indicating that the site-specific nature of this technique is limited.

The retention of tertiary structure was probed through circular dichroism (CD). α-chymotrypsin exhibits a very poor CD signal for characterization in the amide region,(63) therefore CD analysis was undertaken on HLZ and the DTM HLZ conjugate. By recording $\Delta[\theta]_m$ at 222 nm the α-helicity of the enzyme can be measured. A negligible reduction in $[\theta]_{222}$ was noted for the conjugate (97% of the native HLZ – Figure S13) and both CD spectra showed very similar structural features, indicating minimal effect of conjugation on the tertiary structure of HLZ.

For further characterization, the denaturing temperature ($T_m$) was measured for HLZ and the HLZ DTM conjugate for comparison, using differential scanning calorimetry. The $T_m$ for the native enzyme was measured as 72.7 °C in pH 6 buffer, which compares well to previous literature.(64) For the HLZ DTM conjugate, multiple melts were observed (Figure S14), however the major melt can be attributed to the singular DTM HLZ conjugate and was measured at 68.2 °C, suggesting a small loss in thermal stability upon DTM conjugation. The unresolved melts observed below 68.2 °C could be attributed to conjugates with more than one DTM.

To establish whether this technique is suitable for PEGylation, one of the most commonly undertook conjugation procedures, PEG-dibromomaleimide (PEG-

DBM - **1**) was synthesized for use as a conjugation agent. Conjugations were attempted in pH 6 sodium phosphate buffer with a range of DMF concentrations from 0-33% v/v. MALDI-ToF MS analysis for the conjugation of both enzymes to PEG-DBM (**1**) showed that higher DMF concentration lead to higher degrees of PEG conjugation. For α-CT conjugation, 33% v/v DMF conditions gave an average by Gaussian fit of 1.8 attached PEG-DTM molecules (Table 1). The HLZ conjugate however, was observed to have a broader MALDI-ToF mass spectra, where an average of 2.0 PEG-DTMs per enzyme was observed (Table 1).

| Enzyme | Conjugate | # Attached | Conjugation efficiency |
|---|---|---|---|
| **α-CT** | M-DTM | 3/5† | 60 % |
| | PEG-DTM | 1.8 ± 1.5/5 | 36 % |
| **HLZ** | M-DTM | 0-4/4† | ‡ |
| | PEG-DTM | 2.0 ± 1.8/4 | 50 % |

**Table 1.** Table showing number of attached units and conjugation efficiency for disulfide conjugates observed by MALDI-ToF and standard deviation measured by Gaussian fit. †= Gaussian fit not possible, observed conjugates listed. ‡= Quantification not possible.

In order to ascertain whether the conjugated enzymes were fluorescent, excitation and emission spectra were measured for all conjugates of both α-CT and HLZ (for example M-DTM HLZ conjugate in Figure 1B). Table S2, highlights the excitation and emission maxima recorded for the synthesized conjugates (spectra are shown in supporting information 2.1). Emission wavelengths for all conjugates synthesized were similar to those observed in polar solvents for DTM small molecules. (45)

Following this, conjugation utilizing lysine residues was investigated as a novel "turn-on" fluorescence conjugation method. Both enzymes are abundant in lysine residues, with α-CT containing seventeen amine handles for targeting, and HLZ six; this includes three *N*-terminal residues for α-CT and one for HLZ.(52,54) Using M-DBM the conditions of the conjugation were altered to mimic those in the synthesis of ABMs (Figure 2). Conjugating to α-CT overnight, in pH 8.5 buffer, results in a distribution of products as seen at around 26,600 *m/z* by MALDI-ToF MS (see supporting information 1.1.5). By completing a Gaussian fit of this peak an average of 6.2 ± 2.5 ABMs per enzyme is observed. By exposing human lysozyme to the same conditions, successful conjugation was observed by MALDI-ToF MS with an average of 2.7 ± 2.3 ABMs formed per enzyme from six amine handles (Table 2).

The synthesis of smaller MAM dyes has also been reported under these conditions. It was, therefore, decided to synthesize methyl-MBM (**2**), alkyne-MBM (**3**) and PEG-MBM (**4**) for conjugation. The alkyne substituent provides an opportunity for further functionalization, for example *via* copper-catalyzed Huisgen cycloaddition.(25) Conjugation of **2** and **3** was successful for both enzymes and subsequent MALDI-ToF MS analysis showed a distribution of products. Gaussian fits of the spectra are listed in Table 2. The reaction proved much more effective than the ABM reactions showing conjugation of up to 12.1 ± 3.6 MAMs for the α-CT M-MAM conjugate (Figure 2C). PEGylation using **4** was also successful, however lower reactivity was again observed with an average of 2.3 PEG units attached to α-CT and 1.6 to HLZ.

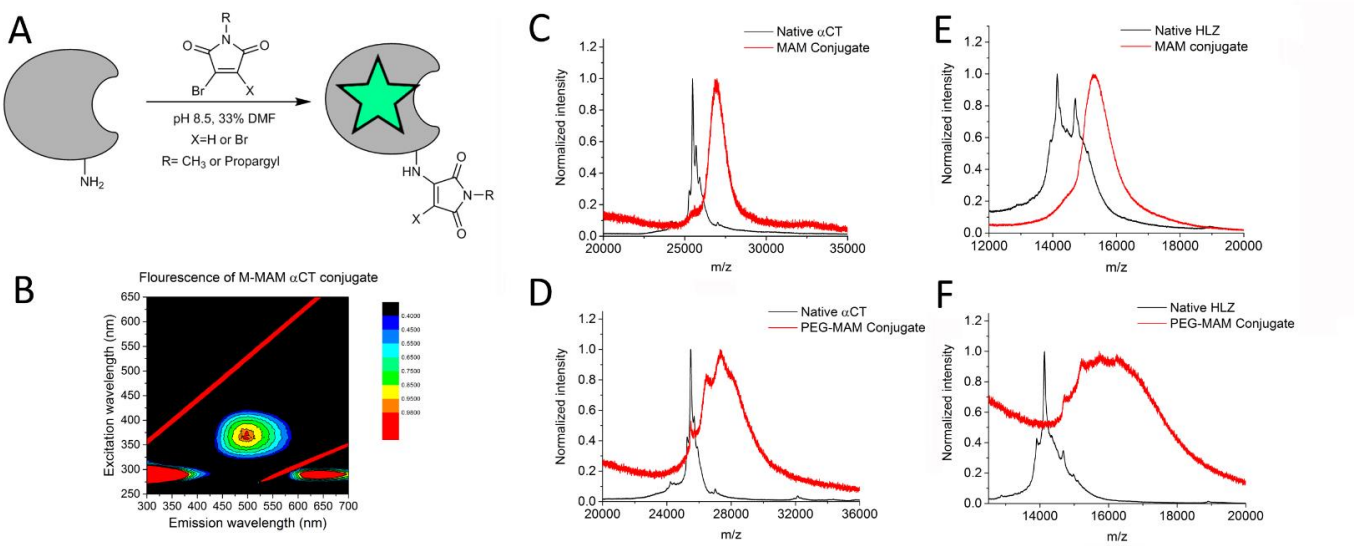


**Figure 2:** (A) Illustration of amine based bromomaleimide conjugations to α-CT and HLZ. (B) 2D excitation–emission spectra of alkyne-MAM HLZ conjugate. MALDI-ToF mass spectra of (C) alkyne-MAM α-CT conjugate (D) PEG-MAM α-CT conjugate (E) alkyne-MAM HLZ conjugate (F) PEG-MAM HLZ conjugate (red) and the native enzyme (black).

| Enzyme | Conjugate | # Attached | Conjugation efficiency |
|---|---|---|---|
| α-CT | M-ABM | 6.2 ± 2.5/17 | 36 % |
| | M-MAM | 12.1 ± 3.6/17 | 71 % |
| | Alkyne-MAM | 11.2 ± 1.8/17 | 66 % |
| | PEG-MAM | 2.3 ± 1.5/17 | 14 % |
| HLZ | M-ABM | 2.7 ± 2.3/6 | 45 % |
| | M-MAM | 5.4 ± 3.1/6 | 90 % |
| | Alkyne-MAM | 4.9 ± 2.5/6 | 82 % |
| | PEG-MAM | 1.5 ± 1.8/6 | 25 % |

**Table 2.** Table showing number of attached units and conjugation efficiency for amine conjugations observed by MALDI-ToF and standard deviation measured by Gaussian fit.

DTM conjugates have been shown to undergo hydrolysis at pH 8.5, dependent on structure, with half-lives as short as 16.5 minutes.(65) In order to ascertain the stability of MAM conjugates, the emission of alkyne-MAM HLZ was studied in pH 8.5 buffer. Under these conditions no hydrolysis was observed over 10 hours (Figure S16), indicating greater resistance to hydrolysis in these MAM species.

Excitation/emission spectra were again measured for all aminomaleimide conjugates of both α-CT and HLZ (for example alkyne-MAM HLZ conjugate in Figure 2) and wavelengths recorded were similar to those observed in water for small molecule species.(45) Small molecule MAMs have been shown to exhibit high (>59 %) quantum yields in organic aprotic solvents, however, in water they are quenched significantly, exhibiting $\Phi_f$<0.4 %.(45) Robin *et al.* have shown that by incorporating DTMs into nanostructures, shielding them from solvent quenching effects, the quantum yield can be restored (>30 %).(39) To investigate whether the same effect would be observed in enzymes, the quantum yield of two conjugates was calculated. The quantum yield of both alkyne-MAM and M-DTM HLZ conjugates was calculated in 18.2 MΩ.cm water, using a standard of quinine ($\Phi_{quinine}$ = 59 %). The alkyne-MAM HLZ conjugate exhibited a quantum yield of $\Phi_f$(%)=0.7 ± 0.04 ($\lambda_{ex}$=362 nm) and the M-DTM HLZ conjugate of $\Phi_f$(%)=0.8 ± 0.07 ($\lambda_{ex}$=365 nm). The quantum yields for both conjugates have increased compared to the DTM and MAM small molecule analogues in water (all less than 0.4 %),(45) however, the values were significantly lower than the fluorescent proteins currently used and would not meet the brightness requirements for applications such as fluorescence microscopy.(66) The quantum yield of the PEGylated HLZ samples were also calculated to compare to the small molecule analogues. The PEG-DTM HLZ conjugate exhibited a quantum yield of $\Phi_f$(%)=0.5 ± 0.05 ($\lambda_{ex}$=362 nm), lower than the respective M-DTM conjugate. This could be attributed to the lower degree of conjugation observed for the polymer species. Theoretically, the most accessible and least shielded disulfide would be the most likely to undergo conjugation, leading to high solvent accessibly, and therefore fluorescence quenching, of the resulting maleimide moiety. In contrast, the PEG-MAM species exhibited a quantum yield of $\Phi_f$(%)=1.4 ± 0.2 ($\lambda_{ex}$=364 nm), double the quantum yield of the respective alkyne-MAM conjugate. In this case, despite exhibiting a lower degree of conjugation compared to the small molecule conjugate, it would appear the polymer chain provides a solvent shielding effect to the MAM dye.

To establish the structural integrity and catalytic activity of the DTM and MAM α-CT conjugates, their activity was measured using a *p*-nitroaniline hydrolysis assay. The initial velocity was measured and compared to the native enzyme at time points.

Results indicated a drop in activity after conjugation for all conjugates (Figure 3A). However it should be noted that the activity is comparable to that of native enzyme left in solution for the time period of the conjugation and purification (6 hours for the DTM conjugates and 24 hours for the MAM conjugates), indicating that the chemical modification itself has negligible effect on enzyme activity, which corroborates the CD analysis for the HLZ DTM conjugate. Positively, stability of the enzyme over 4 days was unaffected (Figure 3B), suggesting the conjugates have similar stability and autolysis rate to the native enzyme.

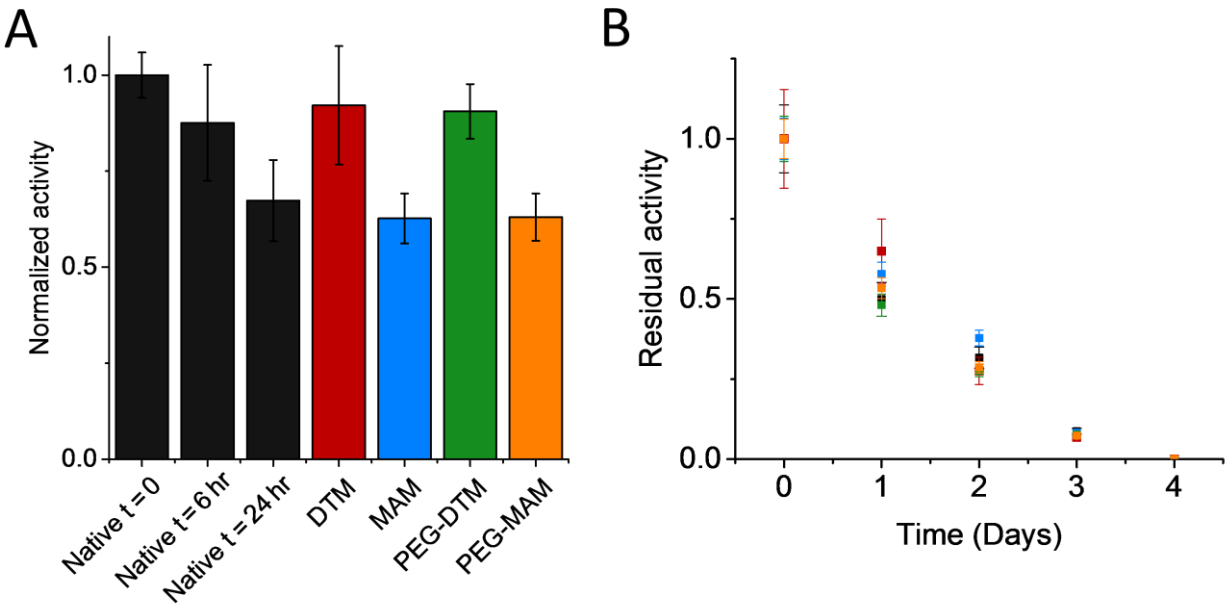


**Figure 3**: (A) Initial activity of α-CT at time points against purified conjugates at t = 0 hr and (B) residual activities of native α-CT and conjugates (black = native enzyme; red = M-DTM conjugate; blue = alkyne-MAM conjugate; green = PEG-DTM conjugate; yellow = PEG-MAM conjugate).

The HLZ conjugates were assayed by EnzChek® lysis to confirm their integrity. This assay relies on the lysis of fluorescein labelled *micrococcus lysodeikticus* cells, where upon cell lysis fluorescence signal increases.(60) When stored at room temperature the conjugates show no discernable difference in activity compared to native HLZ (Figure 4A). To discern whether any differences in stability are observed in more extreme conditions, the conjugates were also examined at 50 °C, and their activity was measured at various time intervals. It has been shown that under raised temperature storage, the stability of native HLZ is negatively affected.(55) Results showed that the MAM conjugates showed a decrease in activity over 7 days comparable to that of the native enzyme. On the other hand, the DTM conjugates

exhibited a decrease in activity. Specifically, the M-DTM conjugate lost all activity over 9 days compared to the native enzyme which retained 44% activity (Figure 4B). This indicates that disulfide re-bridging negatively affected enzyme stability at raised temperature, with the M-DTM conjugate, having the most DTM bridged disulfides, being least stable.

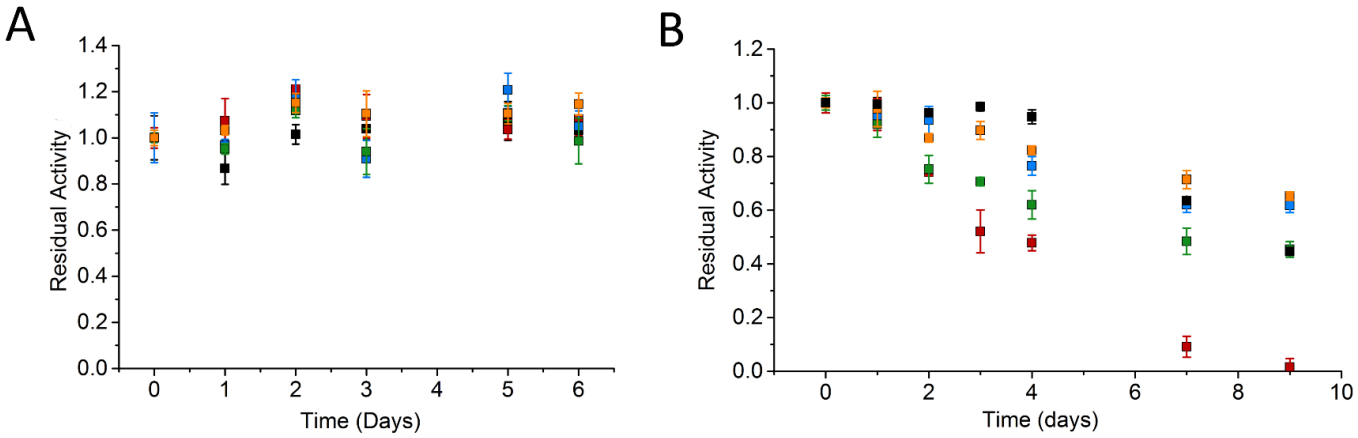


**Figure 4:** The residual activity, by EnzChek® lysis assay, of native HLZ and conjugates when stored at (A) room temperature (B) 50 °C (black = native enzyme; red = M-DTM conjugate; blue = alkyne-MAM conjugate; green = PEG-DTM conjugate; yellow = PEG-MAM conjugate).

## CONCLUSIONS

In conclusion, enzyme conjugates have been synthesized by reacting dibromomaleimides and monobromomaleimides with reduced disulfides and free amines in human lysozyme and α-chymotrpysin. Reactions of dibromomaleimides with reduced disulfides produced dithiomaleimide bridged enzyme conjugates, which showed fluorescence upon formation. Both α-CT and HLZ DTM conjugates showed the same stability as the native enzyme when stored at room temperature, and exhibited negligible structural change by circular dichroism. However, at elevated temperature storage (50 °C) the HLZ DTM conjugates showed reduced stability, which corroborates a decrease in observed $T_{m,}$ indicating this conjugation technique may have a de-stabilizing effect on some enzymes.

Reactions of dibromo- and monobromomaleimides with free amines in both enzymes produced fluorescent aminobromo- and monoaminomaleimide conjugates respectively. Monoaminomaleimides are shown to react with higher efficiency in both enzymes and conjugates are shown to be as stable as native enzymes at room temperature and at 50 °C, however a decrease in $T_m$ was observed by DSC. Fluorescence analysis of all conjugated enzymes showed excitation and emission profiles comparable to small molecule studies, however fluorescence quantum yields were low as a consequence of solvent quenching effects.

Both reactions were trialed as PEGylation methods using bromomaleimide functionalized PEG. Conjugation efficiency was detrimentally effected, attributed to the reduced availability of chain ends and steric hindrance. While, the PEG-MAM HLZ conjugate showed marginally increased fluorescence quantum yield attributed to solvent shielding effects of the short PEG chain.

## ACKNOWLEDGEMENTS

The authors thank Unilever and the ERC for support (grant number: 615142). Malin Suurkuusk (TA instruments) is thanked for DSC analysis.

## REFERENCES

1. Watson P, Jones AT, Stephens DJ. Intracellular trafficking pathways and drug delivery: fluorescence imaging of living and fixed cells. Adv Drug Deliv Rev. 2005 Jan 2;57(1):43–61.

2. Wersto RP, Rosenthal ER, Crystal RG, Spring KR. Uptake of fluorescent dyes associated with the functional expression of the cystic fibrosis transmembrane conductance regulator in epithelial cells. Proc Natl Acad Sci U S A. 1996 Feb 6;93(3):1167–72.

3. Roberti MJ, Jovin TM, Jares-Erijman E. Confocal Fluorescence Anisotropy and FRAP Imaging of α-Synuclein Amyloid Aggregates in Living Cells. PLOS ONE. 2011 Aug 8;6(8):e23338.

4. Wang K, Sachdeva A, Cox DJ, Wilf NM, Lang K, Wallace S, et al. Optimized orthogonal translation of unnatural amino acids enables spontaneous protein double-labelling and FRET. Nat Chem. 2014 May;6(5):393–403.

5. Kajihara D, Abe R, Iijima I, Komiyama C, Sisido M, Hohsaka T. FRET analysis of protein conformational change through position-specific incorporation of fluorescent amino acids. Nat Methods N Y. 2006 Nov;3(11):923–9.

6. Royer CA. Probing Protein Folding and Conformational Transitions with Fluorescence. Chem Rev. 2006 May 1;106(5):1769–84.

7. Yang M, Song Y, Zhang M, Lin S, Hao Z, Liang Y, et al. Converting a Solvatochromic Fluorophore into a Protein-Based pH Indicator for Extreme Acidity. Angew Chem Int Ed. 2012 Jul 27;51(31):7674–9.

8. Sato M, Ozawa T, Inukai K, Asano T, Umezawa Y. Fluorescent indicators for imaging protein phosphorylation in single living cells. Nat Biotechnol. 2002 Mar;20(3):287–94.

9. Henderson JN, Ai H, Campbell RE, Remington SJ. Structural basis for reversible photobleaching of a green fluorescent protein homologue. Proc Natl Acad Sci. 2007 Apr 17;104(16):6672–7.

10. Borrmann A, Milles S, Plass T, Dommerholt J, Verkade JMM, Wießler M, et al. Genetic Encoding of a Bicyclo[6.1.0]nonyne-Charged Amino Acid Enables Fast Cellular Protein Imaging by Metal-Free Ligation. ChemBioChem. 2012 Sep 24;13(14):2094–9.

11. Ariyasu S, Hayashi H, Xing B, Chiba S. Site-Specific Dual Functionalization of Cysteine Residue in Peptides and Proteins with 2-Azidoacrylates. Bioconjug Chem. 2017 Apr 19;28(4):897–902.

12. Ratner V, Kahana E, Eichler M, Haas E. A General Strategy for Site-Specific Double Labeling of Globular Proteins for Kinetic FRET Studies. Bioconjug Chem. 2002 Sep 1;13(5):1163–70.

13. Sachdeva A, Wang K, Elliott T, Chin JW. Concerted, Rapid, Quantitative, and Site-Specific Dual Labeling of Proteins. J Am Chem Soc. 2014 Jun 4;136(22):7785–8.

14. Nguyen DP, Elliott T, Holt M, Muir TW, Chin JW. Genetically Encoded 1,2-Aminothiols Facilitate Rapid and Site-Specific Protein Labeling via a Bio-orthogonal Cyanobenzothiazole Condensation. J Am Chem Soc. 2011 Aug 3;133(30):11418–21.

15. Plass T, Milles S, Koehler C, Szymański J, Mueller R, Wießler M, et al. Amino Acids for Diels–Alder Reactions in Living Cells. Angew Chem Int Ed. 2012 Apr 23;51(17):4166–70.

16. Stephanopoulos N, Francis MB. Choosing an effective protein bioconjugation strategy. Nat Chem Biol. 2011 Dec;7(12):876–84.

17. Suzuki T, Kanbara N, Tomono T, Hayashi N, Shinohara I. Physicochemical and biological properties of poly(ethylene glycol)-coupled immunoglobuling G. Biochim Biophys Acta BBA - Protein Struct Mol Enzymol. 1984 Jul 31;788(2):248–55.

18. Cao S-G, Zhao Q, Ding Z-T, Ma L, Yu T, Wang J-H, et al. Chemical Modification of Enzyme Molecules to Improve Their Characteristics. Ann N Y Acad Sci. 1990 Dec 1;613(1):460–7.

19. Chen RH-L, Abuchowski A, Van Es T, Palczuk NC, Davis FF. Properties of two urate oxidases modified by the covalent attachment of poly(ethylene glycol). Biochim Biophys Acta BBA - Enzymol. 1981 Aug 13;660(2):293–8.

20. Kurtzberg J, Asselin B, Bernstein M, Buchanan GR, Pollock BH, Camitta BM. Polyethylene Glycol-conjugated L-asparaginase versus native L-asparaginase in combination with standard agents for children with acute lymphoblastic leukemia in second bone marrow relapse: a Children's Oncology Group Study (POG 8866). J Pediatr Hematol Oncol. 2011 Dec;33(8):610–6.

21. Tsutsumi Y, Kihira T, Tsunoda S, Kanamori T, Nakagawa S, Mayumi T. Molecular design of hybrid tumour necrosis factor alpha with polyethylene glycol increases its anti-tumour potency. Br J Cancer. 1995 May;71(5):963–8.

22. Alconcel SNS, Baas AS, Maynard HD. FDA-approved poly(ethylene glycol)–protein conjugate drugs. Polym Chem. 2011 Jun 14;2(7):1442–8.

23. Schelté P, Boeckler C, Frisch B, Schuber F. Differential Reactivity of Maleimide and Bromoacetyl Functions with Thiols: Application to the Preparation of Liposomal Diepitope Constructs. Bioconjug Chem. 2000 Jan 1;11(1):118–23.

24. Stenzel MH. Bioconjugation Using Thiols: Old Chemistry Rediscovered to Connect Polymers with Nature's Building Blocks. ACS Macro Lett. 2013 Jan 15;2(1):14–8.

25. Li M, De P, Gondi SR, Sumerlin BS. Responsive Polymer-Protein Bioconjugates Prepared by RAFT Polymerization and Copper-Catalyzed Azide-Alkyne Click Chemistry. Macromol Rapid Commun. 2008 Jul 1;29(12-13):1172–6.

26. Bays E, Tao L, Chang C-W, Maynard HD. Synthesis of Semitelechelic Maleimide Poly(PEGA) for Protein Conjugation By RAFT Polymerization. Biomacromolecules. 2009 Jul 13;10(7):1777–81.

27. Yang SK, Shi X, Park S, Doganay S, Ha T, Zimmerman SC. Monovalent, Clickable, Uncharged, Water-Soluble Perylenediimide-Cored Dendrimers for Target-Specific Fluorescent Biolabeling. J Am Chem Soc. 2011 Jul 6;133(26):9964–7.

28. Fujita Y, Murakami Y, Noda A, Miyoshi S. Design and Synthesis of an Easily Obtainable Maleimide Reagent N-[2-(4-[18F]fluoro-N-methylbenzenesulfonamido)ethyl]maleimide ([18F]FBSEM) to Radiolabel Thiols in Proteins. Bioconjug Chem. 2017 Feb 15;28(2):642–8.

29. Tedaldi LM, Smith MEB, Nathani RI, Baker JR. Bromomaleimides: new reagents for the selective and reversible modification of cysteine. Chem Commun. 2009 Oct 28;(43):6583–5.

30. Smith MEB, Schumacher FF, Ryan CP, Tedaldi LM, Papaioannou D, Waksman G, et al. Protein Modification, Bioconjugation, and Disulfide Bridging Using Bromomaleimides. J Am Chem Soc. 2010 Feb 17;132(6):1960–5.

31. Schumacher FF, Nunes JPM, Maruani A, Chudasama V, Smith MEB, Chester KA, et al. Next generation maleimides enable the controlled assembly of antibody–drug conjugates via native disulfide bond bridging. Org Biomol Chem. 2014 Aug 27;12(37):7261–9.

32. Castañeda L, Maruani A, Schumacher FF, Miranda E, Chudasama V, Chester KA, et al. Acid-cleavable thiomaleamic acid linker for homogeneous antibody–drug conjugation. Chem Commun. 2013 Aug 20;49(74):8187–9.

33. Hull EA, Livanos M, Miranda E, Smith MEB, Chester KA, Baker JR. Homogeneous Bispecifics by Disulfide Bridging. Bioconjug Chem. 2014 Aug 20;25(8):1395–401.

34. Nunes JPM, Morais M, Vassileva V, Robinson E, Rajkumar VS, Smith MEB, et al. Functional native disulfide bridging enables delivery of a potent, stable and targeted antibody–drug conjugate (ADC). Chem Commun. 2015 Jun 18;51(53):10624–7.

35. Robin MP, Wilson P, Mabire AB, Kiviaho JK, Raymond JE, Haddleton DM, et al. Conjugation-Induced Fluorescent Labeling of Proteins and Polymers Using Dithiomaleimides. J Am Chem Soc. 2013 Feb 27;135(8):2875–8.

36. Collins J, Tanaka J, Wilson P, Kempe K, Davis TP, McIntosh MP, et al. In Situ Conjugation of Dithiophenol Maleimide Polymers and Oxytocin for Stable and Reversible Polymer–Peptide Conjugates. Bioconjug Chem. 2015 Apr 15;26(4):633–8.

37. Collins J, Kempe K, Wilson P, Blindauer CA, McIntosh MP, Davis TP, et al. Stability Enhancing N-Terminal PEGylation of Oxytocin Exploiting Different Polymer Architectures and Conjugation Approaches. Biomacromolecules. 2016 Aug 8;17(8):2755–66.

38. Grison CM, Burslem GM, Miles JA, Pilsl LKA, Yeo DJ, Imani Z, et al. Double quick, double click reversible peptide “stapling.” Chem Sci. 2017 Jun 26;8(7):5166–71.

39. Robin MP, Mabire AB, Damborsky JC, Thom ES, Winzer-Serhan UH, Raymond JE, et al. New Functional Handle for Use as a Self-Reporting Contrast and Delivery Agent in Nanomedicine. J Am Chem Soc. 2013 Jun 26;135(25):9518–24.

40. Robin MP, O'Reilly RK. Fluorescent and chemico-fluorescent responsive polymers from dithiomaleimide and dibromomaleimide functional monomers. Chem Sci. 2014 Jun 3;5(7):2717–23.

41. Mabire AB, Robin MP, Willcock H, Pitto-Barry A, Kirby N, O'Reilly RK. Dual effect of thiol addition on fluorescent polymeric micelles: ON-to-OFF emissive switch and morphology transition. Chem Commun. 2014 Sep 4;50(78):11492–5.

42. Tang Z, Wilson P, Kempe K, Chen H, Haddleton DM. Reversible Regulation of Thermoresponsive Property of Dithiomaleimide-Containing Copolymers via Sequential Thiol Exchange Reactions. ACS Macro Lett. 2016 Jun 21;5(6):709–13.

43. Robin MP, O'Reilly RK. Strategies for preparing fluorescently labelled polymer nanoparticles. Polym Int. 2015 Feb 1;64(2):174–82.

44. Robin MP, Osborne SAM, Pikramenou Z, Raymond JE, O'Reilly RK. Fluorescent Block Copolymer Micelles That Can Self-Report on Their Assembly and Small Molecule Encapsulation. Macromolecules. 2016 Jan 26;49(2):653–62.

45. Mabire AB, Robin MP, Quan W-D, Willcock H, Stavros VG, O'Reilly RK. Aminomaleimide fluorophores: a simple functional group with bright, solvent dependent emission. Chem Commun. 2015 Jun 14;51(47):9733–6.

46. Imoto H, Nohmi K, Kizaki K, Watase S, Matsukawa K, Yamamoto S, et al. Effect of alkyl groups on emission properties of aggregation induced emission active N-alkyl arylaminomaleimide dyes. RSC Adv. 2015;5(114):94344–50.

47. Kato T, Naka K. Arylaminomaleimides as a New Class of Aggregation-induced Emission-active Molecules Obtained from Organoarsenic Compounds. Chem Lett. 2012;41(11):1445–7.

48. Hermanson GT. Chapter 3 - The Reactions of Bioconjugation. In: Bioconjugate Techniques (Third edition) [Internet]. Boston: Academic Press; 2013 [cited 2016 Jul 21]. p. 229–58. Available from: http://www.sciencedirect.com/science/article/pii/B9780123822390000030

49. Jung D, Min K, Jung J, Jang W, Kwon Y. Chemical biology-based approaches on fluorescent labeling of proteins in live cells. Mol Biosyst. 2013 Apr 2;9(5):862–72.

50. Jones MW, Strickland RA, Schumacher FF, Caddick S, Baker JR, Gibson MI, et al. Highly efficient disulfide bridging polymers for bioconjugates from radical-compatible dithiophenol maleimides. Chem Commun. 2012 Mar 28;48(34):4064–6.

51. Cummings C, Murata H, Koepsel R, Russell AJ. Tailoring enzyme activity and stability using polymer-based protein engineering. Biomaterials. 2013 Oct;34(30):7437–43.

52. Tsukada H, Blow DM. Structure of alpha-chymotrypsin refined at 1.68 A resolution. J Mol Biol. 1985 Aug 20;184(4):703–11.

53. Falatach R, Li S, Sloane S, McGlone C, Berberich JA, Page RC, et al. Why synthesize protein–polymer conjugates? The stability and activity of chymotrypsin-polymer bioconjugates synthesized by RAFT. Polymer. 2015 Aug 18;72:382–6.

54. Artymiuk PJ, Blake CCF. Refinement of human lysozyme at 1.5 Å resolution analysis of non-bonded and hydrogen-bond interactions. J Mol Biol. 1981 Nov 15;152(4):737–62.

55. Avanti C, Saluja V, Streun ELP van, Frijlink HW, Hinrichs WLJ. Stability of Lysozyme in Aqueous Extremolyte Solutions during Heat Shock and Accelerated Thermal Conditions. PLOS ONE. 2014 Jan 23;9(1):e86244.

56. Dumoulin M, Johnson RJK, Bellotti V, Dobson CM. Human Lysozyme. In: Uversky VN, Fink AL, editors. Protein Misfolding, Aggregation, and Conformational Diseases. Springer US; 2007. p. 285–308. (Protein Reviews).

57. Liu M, Tirino P, Radivojevic M, Phillips DJ, Gibson MI, Leroux J-C, et al. Molecular Sieving on the Surface of a Protein Provides Protection Without Loss of Activity. Adv Funct Mater. 2013 Apr 25;23(16):2007–15.

58. Cummings CS, Campbell AS, Baker SL, Carmali S, Murata H, Russell AJ. Design of Stomach Acid-Stable and Mucin-Binding Enzyme Polymer Conjugates. Biomacromolecules. 2017 Feb 13;18(2):576–86.

59. Smith MEB, Caspersen MB, Robinson E, Morais M, Maruani A, Nunes JPM, et al. A platform for efficient, thiol-stable conjugation to albumin's native single accessible cysteine. Org Biomol Chem. 2015 Jul 16;13(29):7946–9.

60. Helal R, Melzig MF. Determination of lysozyme activity by a fluorescence technique in comparison with the classical turbidity assay. Pharm - Int J Pharm Sci. 2008 Jun 1;63(6):415–9.

61. Würth C, Grabolle M, Pauli J, Spieles M, Resch-Genger U. Relative and absolute determination of fluorescence quantum yields of transparent samples. Nat Protoc. 2013 Aug;8(8):1535–50.

62. Zhang Q, Li M, Zhu C, Nurumbetov G, Li Z, Wilson P, et al. Well-Defined Protein/Peptide–Polymer Conjugates by Aqueous Cu-LRP: Synthesis and Controlled Self-Assembly. J Am Chem Soc. 2015 Jul 29;137(29):9344–53.

63. Jibson MD, Birk Y, Bewley TA. Circular Dichroism Spectra of Trypsin and Chymotrypsin Complexes with Bowman-Birk or Chickpea Trypsin Inhibitor. Int J Pept Protein Res. 1981 Jul 1;18(1):26–32.

64. Booth DR, Sunde M, Bellotti V, Robinson CV, Hutchinson WL, Fraser PE, et al. Instability, unfolding and aggregation of human lysozyme variants underlying amyloid fibrillogenesis. Nature. 1997 Feb;385(6619):787.

65. Morais M, Nunes JPM, Karu K, Forte N, Benni I, Smith MEB, et al. Optimisation of the dibromomaleimide (DBM) platform for native antibody conjugation by accelerated post-conjugation hydrolysis. Org Biomol Chem. 2017 Apr 5;15(14):2947–52.

66. Shaner NC, Steinbach PA, Tsien RY. A guide to choosing fluorescent proteins. Nat Methods. 2005 Dec;2(12):905–9.

## TABLES

| Enzyme | Conjugate | # Attached | Conjugation efficiency |
|---|---|---|---|
| α-CT | M-DTM | 3/5† | 60 % |
| | PEG-DTM | 1.8 ± 1.5/5 | 36 % |
| HLZ | M-DTM | 0-4/4† | ‡ |
| | PEG-DTM | 2.0 ± 1.8/4 | 50 % |

**Table 1.** Table showing number of attached units and conjugation efficiency for disulfide conjugates observed by MALDI-ToF and standard deviation measured by Gaussian fit. †= Gaussian fit not possible, observed conjugates listed. ‡= Quantification not possible.

| Enzyme | Conjugate | # Attached | Conjugation efficiency |
|---|---|---|---|
| α-CT | M-ABM | 6.2 ± 2.5/17 | 36 % |
| | M-MAM | 12.1 ± 3.6/17 | 71 % |
| | Alkyne-MAM | 11.2 ± 1.8/17 | 66 % |
| | PEG-MAM | 2.3 ± 1.5/17 | 14 % |
| HLZ | M-ABM | 2.7 ± 2.3/6 | 45 % |
| | M-MAM | 5.4 ± 3.1/6 | 90 % |
| | Alkyne-MAM | 4.9 ± 2.5/6 | 82 % |
| | PEG-MAM | 1.5 ± 1.8/6 | 25 % |

**Table 2.** Table showing number of attached units and conjugation efficiency for amine conjugations observed by MALDI-ToF and standard deviation measured by Gaussian fit.

## FIGURE LEDGENDS

**Figure 1:** (A) Illustration of disulfide based bromomaleimide conjugations to α-CT and HLZ. (B) 2D excitation–emission spectra of M-DTM HLZ conjugate. MALDI-ToF mass spectra of (C) M-DTM α-CT conjugate (D) PEG-DTM α-CT conjugate (E) M-DTM HLZ conjugate (F) PEG-DTM HLZ conjugate (red) with the native enzyme (black).

**Figure 2:** (A) Illustration of amine based bromomaleimide conjugations to α-CT and HLZ. (B) 2D excitation–emission spectra of alkyne-MAM HLZ conjugate. MALDI-ToF mass spectra of (C) alkyne-MAM α-CT conjugate (D) PEG-MAM α-CT conjugate (E)

alkyne-MAM HLZ conjugate (F) PEG-MAM HLZ conjugate (red) and the native enzyme (black).

**Figure 3**: (A) Initial activity of α-CT at time points against purified conjugates at t = 0 hr and (B) residual activities of native α-CT and conjugates (black = native enzyme; red = M-DTM conjugate; blue = alkyne-MAM conjugate; green = PEG-DTM conjugate; yellow = PEG-MAM conjugate).

**Figure 4:** The residual activity, by EnzChek® lysis assay, of native HLZ and conjugates when stored at (A) room temperature (B) 50 °C (black = native enzyme; red = M-DTM conjugate; blue = alkyne-MAM conjugate; green = PEG-DTM conjugate; yellow = PEG-MAM conjugate).